Hydrophobic Acceleration of Electron-Transfer Fluorescence Quenching Processes between Excited 1-Alkanoylperylenes and Ferrocene Derivatives

SHI, Ji-Liang* (史济良) **XU, Jia-Yi**(许家移) **JIANG, Xi-Kui**(蒋锡夔)

Shanghai Institute of Organic Chemistry, Chinese Academy of Sciences, Shanghai 200032, China

Coaggregation-facilitated Electron-transfer (ET) fluorescence quenching processes between an excited 1-alkanoylperylene (Pe-*n*, *n* = 4, 8, 12) as an acceptor and an 1-alkanoylferrocene (Fc-*m*, *m* = 4, 8, 12, 16) or a 1,1-dialkanoylferrocene (Fc-*m*-2, *m* = 4, 8, 12, 16) as a donor have been investigated by means of fluorescence spectroscopy in dioxane (DX)-H_2O binary solvents of different Φ values, where Φ is the volume fraction of the organic component of an aquiorgano mixture. This is a first observation of an ET processes facilitated by hydrophobic-lipophilic interaction (HLI) with organometallic compounds as donors. The extent of HLI-driven coaggregation between the acceptor and the donor may be assessed from the efficiency of fluorescence quenching, *i. e.*, the slope B of Eq. (2). The chain-foldability effect and the intramolecular "self-satisfaction" of HLI for Fc-*m*-2 have been observed. The experimental results show that the behavior of Fc-*m* as a quencher for fluorescence quenching of Pe-*n is rather similar to that of *N*-alkylsubstituend phenothiazine.**

Keywords Excited alkanoyl perylene, hydrophobic acceleration of electron-transfer, coaggregation, fluorescence quenching, alkanoyl ferrocene

Photoinduced intramolecular and intermolecular electron-transfer (ET) processes as a mean of capturing and storing solar energy have attracted the attention of many chemists.[1-3] These processes are also of interest in supramolecular chemistry.[4] Recently, Guldi *et al.* reported intramolecular ET in fullerene/ferrocene based donor-bridge-acceptor dyads.[5] ET fluorescence quenching processes brought about by coaggregation under the influence of hydrophobic-lipophilic interaction (HLI),[6-8] have been investigated previously. We now extend our research to systems with excited perylene derivative (**Pe-*n***) as acceptors and ferrocene derivatives (**Fc-*m*** and **Fc-*m*-2**)[9,10] as donors. One of the simplest and most characteristic reactions of ferrocene is the ET oxidation reaction. Fluorescence quenching results have demonstrated the occurrence of coaggregation of two aggregators under the influence of HLI. The "proximity" effect of HLI-enforced coaggregation and self-coiling of organic compounds may have valuable applications to the study of photoinduced intermolecular and intramolecular ET processes because the photoinduced ET process is strongly dependent on the distance between the excited acceptor (or donor) and the electron donor (or acceptor). Furthermore, in polar solvents the free energy change of ET can be given by the Weller equation, and for above-mentioned systems the changes of free energy are negative. This indicates that the ET fluorescence quenching process between **Pe-*n**** and the donor should occur spontaneously when the proximity effect is operating. However, at low concentrations of **Pe-*n**** and the donor ($< 10^{-6}$ mol/L) in pure dioxane there is no fluorescence quenching because of the absence of HLI in pure dioxane. In other words, for the HLI accelerated ET fluorescence quenching process, the key factor is the proximity effect derived from coaggregation of the acceptor and the donor.

Compounds used in this study are 1-alkanoylperylene (**Pe-*n***, *n* = 4, 8, 12), 1-alkanoylferrocene (**Fc-*m***, *m* = 4, 8, 12, 16), 1,1-dialkanoylferrocene (**Fc-*m*-2**, *m* = 4, 8, 12, 16) and *N*-dodecylphenothiazine

* E-mail: jxk@pub.sioc.ac.cn

Received September 29, 2000; revised November 24, 2000; accepted December 12, 2000.

(**PTZ-12**).

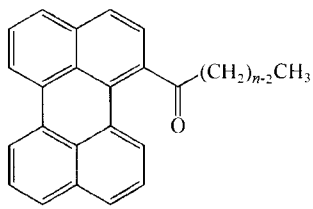

Pe-*n* (*n*=4, 8, 12)

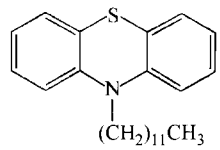

PTZ-12

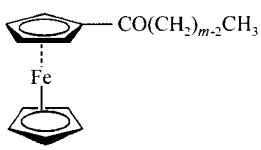

Fc-*m* (*m*=4, 8, 12, 16)

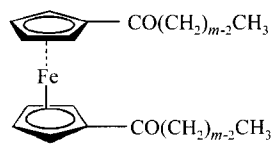

Fc-*m*-2 (*m*=4, 8, 12, 16)

Experimental

Apparatus

^{1}H NMR spectra were obtained at 90 MHz on a Varian FX-90 Q spectrometer with TMS as the internal standard. Mass spectra were obtained by using an HP 5989A spectrometer at an ionization potential of 70 eV. UV-Vis spectra were recorded by using Perkin-Elmer Lambda 2 spectrometer. Melting points were not corrected.

Fluorescence spectra

All aquiorgano solutions used for spectroscopic measurements were prepared from deionized water and dioxane (DX) that was purified by a standard procedure.[11] Fluorescence emission spectra in aquiorgano solutions (DX-H_2O) of **Pe-*n*** * or **Pe-*n*** * and the donor were recorded by a Perkin-Elmer LS-50 spectrometer at λ_{ex} = 446 nm and 35℃. The experimental uncertainty in fluorescence intensity measurements was less than 5%, but, in the measurements of B values, the experimental uncertainty was ± 10%.

In above-mentioned results, the ε value of **Fc**-12 was 3.7×10^2 mol^{-1}·L·cm^{-1} at 446 nm, and the ε value of **Fc**-12-**2** was 4.7×10^2 mol^{-1}·L·cm^{-1} at 459 nm, but, the ε value of **Pe**-12 was 2.5×10^4 mol^{-1}·L·cm^{-1} at 446 nm.[13] In other words, at 446 nm the ε value of **Fc**-12 or **Fc**-12-**2** is only about 1% of the ε value of **Pe**-12. Therefore, the absorptive interference by **Fc-*m*** or **Fc-*m*-2** in the excited experiments of **Pe-*n*** at 446 nm was negligible in the experimental assessment of uncertainty.

Reagents and substrates

The samples of **Pe-*n***, **Fc-*m*** and **Fc-*m*-2** were prepared by the Friedel-Crafts reaction in refluxed 1,2-dichloroethane. These samples were purified by flash column choromatography on silica gel with CCl_4-CH_2Cl_2 as the eluent. The ^{1}H NMR results of the samples suggest that the alkanoyl group is at 1-position and it is not at 3-position. It is consistent with the result reported in the literature.[12] Compounds **Pe-*n*** and **PTZ-12** have been reported elsewhere.[13,14] **Fc-*m*** and **Fc-*m*-2** are new compounds. They were identified by ^{1}H NMR, elemental analysis and mass spectral data. The corresponding data for **Fc-*m*** and **Fc-*m*-2** are reported below.

Butyrylferrocene (**Fc**-4) Deeply red liquid; ^{1}H NMR ($CDCl_3$) δ: 0.90 (t, $J_1 = J_2 = 6.0$ Hz, 3H), 1.63—1.86 (m, 2H), 2.70 (t, $J_1 = J_2 = 6.0$ Hz, 2H), 4.20 (s, 5H), 4.45—4.56 (m, 2H), 4.85—4.89 (m, 2H); UV-Vis (1,4-dioxane): 268, 446 nm; MS(ET, *m/z*(%): 185 (38.30), 186 (12.40), 213 (30.94), 228 (7.42), 256 (100.00, M^+), 257 (17.30, $M^+ + 1$); Anal. Calcd for $C_{14}H_{16}OFe$: C 65.65, H 6.30; found: C 65.35, H 6.35.

Octanoylferrocene (**Fc**-8) Deeply red liquid; ^{1}H NMMR ($CDCl_3$) δ: 0.90 (t, $J_1 = J_2 = 6.0$ Hz, 3H), 1.18—1.46 (m, 8H), 1.63—1.76 (m, 2H), 2.70 (t, $J_1 = J_2 = 6.0$ Hz, 2H), 4.20 (s, 5H), 4.44—4.56 (m, 2H), 4.84—4.89 (m, 2H); UV-Vis (1, 4-dioxane) λ_{max}: 268, 446 nm; MS (*m/z* (%): 185 (23.95), 186 (18.33), 213 (18.18), 228 (39.38), 312 (100.00, M^+), 313 (21.07, $M^+ + 1$); Anal. Calcd for $C_{18}H_{24}OFe$: C 69.24, H 7.75; found: C 69.27, H 7.82.

Lauroylferrocene (**Fc**-12) Red solid, m.p. 46.5—47.5℃; ^{1}H NMR ($CDCl_3$) δ: 0.90 (t, $J_1 = J_2 = 5.4$ Hz, 3H), 1.23—1.38 (m, 16H), 1.62—1.74 (m, 2H), 2.70 (t, $J_1 = J_2 = 6.0$ Hz, 2H), 4.20 (s, 5H), 4.45—4.57 (m, 2H), 4.83—4.88 (m, 2H); UV-Vis (1,4-dioxane) λ_{max}: 268 ($\varepsilon = 6.4 \times 10^3$ mol^{-1}·L·cm^{-1}), 446 ($\varepsilon = 3.7 \times 10^2$ mol^{-1}·L) nm; MS (ET) *m/z* (%): 185 (15.34), 186 (15.22), 213

(10.47), 228 (23.31), 368 (110.00, M^+), 369 (27.09, $M^+ + 1$); Anal. Calcd for $C_{22}H_{32}OFe$: C 71.74, H 8.76; found: C 71.73, H 8.76.

Palmitoylferrocene (**Fc-16**) Red solid, m.p. 63—64. ^1H NMR ($CDCl_3$) δ: 0.90 (t, $J_1 = J_2 = 5.4$ Hz, 3H), 1.17—1.45 (m, 24H), 1.63—1.76 (m, 2H), 2.70 (t, $J_1 = J_2 = 7.2$ Hz, 2H), 4.20 (s, 5H), 4.44—4.56 (m, 2H), 4.85—4.90 (m, 2H); UV-Vis (1,4-dioxane) λ_{max}: 268, 446 nm; MS (ET) *m/z*(%): 185 (9.68), 186 (12.16), 213 (6.02), 228 (13.57), 424 (100.00, M^+), 425 (30.97, $M^+ + 1$); Anal. Calcd for $C_{26}H_{40}OFe$: C 73.57, H 9.50; found: C 73.63, H 9.50.

1,1′-*Dibutyrylferrocene* (**Fc-4-2**) Red solid, m.p. 78—79℃; ^1H NMR ($CDCl_3$) δ: 1.00 (t, $J_1 = J_2 = 6.6$ Hz, 6H), 1.68—1.72 (m, 4H), 4.00 (s, 4H), 4.60 (s, 4H); UV-Vis (1,4-dioxane) λ_{max}: 262 ($\varepsilon = 1.3 \times 10^4$ $mol^{-1} \cdot L \cdot cm^{-1}$), 326 ($\varepsilon = 1.8 \times 10^3$ $mol^{-1} \cdot L \cdot cm^{-1}$), 459 ($\varepsilon = 4.5 \times 10^2$ $mol^{-1} \cdot L \cdot cm^{-1}$) nm; MS (ET) *m/z*(%): 185 (14.37), 186 (12.12), 213 (14.77), 282 (27.37), 297 (4.95), 326 (100.00, M^+), 327 (23.46, $M^+ + 1$); Anal. Calcd for $C_{18}H_{22}O_2Fe$: C 66.27, H 6.80; found: C 66.34, H 6.95.

1,1′-*Dioctanoylferrocene* (**Fc-8-2**) Red needle crystal, m.p. 62—63℃; ^1H NMR ($CDCl_3$) δ: 1.00 (t, $J_1 = J_2 = 4.5$ Hz, 6H), 1.40—2.00 (m, 20H), 2.8 (t, $J_1 = J_2 = 7.5$ Hz, 4H), 4.50 (s, 4H), 4.90 (s, 4H); UV-Vis (1,4-dioxane) λ_{max}: 262 ($\varepsilon = 1.2 \times 10^4$ $mol^{-1} \cdot L \cdot cm^{-1}$), 326 ($\varepsilon = 1.8 \times 10^3$ $mol^{-1} \cdot L \cdot cm^{-1}$), 459 ($\varepsilon = 4.5 \times 10^2$ $mol^{-1} \cdot L \cdot cm^{-1}$) nm; MS (ET) *m/z* (%): 185 (6.34), 186 (12.11), 213 (4.75), 353 (17.43),438 (100.00, M^+), 439 (36.81, $M^+ + 1$); Anal. Calcd for $C_{26}H_{38}O_2Fe$: C 71.23, H 8.74; found: C 71.36, H 8.86.

1,1′-*Dilauroylferrocene* (**Fc-12-2**) Red plate-like crystal, m.p. 81—82℃; ^1H NMR ($CDCl_3$) δ: 0.90 (t, $J_1 = J_2 = 6.0$ Hz, 6H), 1.30 (s, 32H), 1.60—1.80 (m, 4H), 2.70 (t, $J_1 = J_2 = 7.5$ Hz, 4H), 4.45—4.57 (m, 4H), 4.83—4.88 (m, 4H); UV-Vis (1,4-dioxane) λ_{max}: 262 ($\varepsilon = 1.2 \times 10^4$ $mol^{-1} \cdot L \cdot cm^{-1}$), 326 ($\varepsilon = 1.9 \times 10^3$ $mol^{-1} \cdot L \cdot cm^{-1}$), 459 ($\varepsilon = 4.7 \times 10^2$ $mol^{-1} \cdot L \cdot cm^{-1}$) nm. MS (ET) *m/z* (%): 185 (4.11), 186 (7.20), 213 (4.75), 410 (8.81), 550 (100.00, M^+), 551 (51.50, $M^+ + 1$); Anal. Calcd for $C_{34}H_{54}O_2Fe$: C 74.16, H 9.88; found: C 74.18, H 9.70.

1,1′-*Dipalmitoylferrocene* (**Fc-16-2**) Red solid, m.p. 89.5—90.5℃; ^1H NMR ($CDCl_3$) δ: 0.90 (t, $J_1 = J_2 = 5.4$ Hz, 6H), 1.30 (s, 48H), 1.60—1.80 (m, 4H), 2.70 (t, $J_1 = J_2 = 7.5$ Hz, 4H), 4.50 (s, 4H), 4.80 (s, 4H); UV-Vis (1,4-dioxane) λ_{max}: 262 ($\varepsilon = 1.2 \times 10^4$ $mol^{-1} \cdot L \cdot cm^{-1}$), 326 ($\varepsilon = 1.9 \times 10^3$ $mol^{-1} \cdot L \cdot cm^{-1}$), 459 ($\varepsilon = 4.7 \times 10^2$ $mol^{-1} \cdot L \cdot cm^{-1}$) nm; Anal. Calcd for $C_{42}H_{70}O_2Fe$: C 76.20, H 10.64, found: C 76.20, H 10.98.

Results and discussion

Critical aggregate concentrations (CAgCs)[15] of **Pe-*n*** in DX-H_2O mixtures of different Φ values have been measured and reported elsewhere.[14]

When one of the molecules is in its excited state, the free energy change of the ET quenching in polar solvents between the acceptor and the donor can be given by the Weller equation,[16] *i. e.*, $\Delta G = E^{ox}_{1/2} - E^{red}_{1/2} - E_{00}$. The corresponding oxidation potentials of **PTZ-12**, **Fc-*m*** and **Fc-*m*-2** have been measured by cyclic voltammetry in 0.1 mol/L of tetrabutylammonium perchlorate/CH_3CN, *i. e.*, TBA(ClO_4)/CH_3CN. These $E^{ox}_{1/2}$ values (versus SCE) are as follows: 0.674 V for **PTZ-12**; 0.671 V for **Fc-*m***, and 0.886 V for **Fc-*m*-2**. The reduction potential of **Pe-*n*** has also been measured by the above-mentioned method. It is −1.353 V (versus SCE). On the basis of the fact that at $\lambda_{ex} = 446$ nm the energy E_{00} of **Pe-*n*** * is 2.78 eV ($E_{00} = 28600/\lambda_{ex}$) in a polar solvent, application of the Weller equation will give the following ΔG values, namely, i) between **Pe-*n*** * and **PTZ-12**, $\Delta G = [0.674 - (-1.353) - 2.78] \times 23.06 \times 4.186 = -72.67$ kJ/mol; ii) between **Pe-*n*** * and **Fc-*m***, $\Delta G = [0.671 - (-1.353) - 2.78] \times 23.06 \times 4.186 = -72.96$ kJ; iii) between **Pe-*n*** * and **Fc-*m*-2**, $\Delta G = [0.886 - (-1.353) - 2.78] \times 23.06 \times 4.186 = -52.24$ kJ. All the above-mentioned ΔG values are negative. It indicated that the ET fluorescence quenching process between **Pe-*n*** * and donor will occur spontaneously when the proximity effect brought about by coaggregation is operating.

In pure DX, there is no fluorescence quenching between **Pe-*n*** * and the quencher (**PTZ-12** or **Fc-*m*** or **Fc-*m*-2**) at low concentration ($\approx 10^{-7}$ mol/L). Under our experimental conditions, since the concentration of **Pe-*n*** is below its CAgC, the possibility of self-quench-

ing between **Pe-n*** and **Pe-n** can be excluded (*cf.* Ref. 15). Furthermore, when the excitation wavelength of 446 nm was used, there were no fluorescences from **Fc-m**, **Fc-m-2**, and **PTZ-12**. In other words, there could be no interference for the fluorescence measurements of **Pe-n*** from the presence of **Fc-m**, **Fc-m-2**, and **PTZ-12**.

It has been found that when the concentration of the quencher [Q] is smaller than the critical coaggregate concentration (CoCAgC), *i.e.*, [Q] < CoCAgC, the I_0/I_n ratio appears to be independent of [Q] in Eq. (1), where I_0 and I_n represent the fluorescence intensity of **Pe-n*** in the absence and presence of quencher respectively, even though the exact value of this ratio could not be very accurately measured because the quencher concentration was much too dilute. However, at the quencher concentrations $\geq$ CoCAgC, the I_0/I_n plot is a straight line with the slope B, as exemplified by Fig. 1 and Fig. 2. B value shows the efficiency of the coaggregation fluorescence quenching and a larger B value signifies more effective fluorescence quenching. A was found to be unity, with an uncertainty of ± 10%. A total of about 100 I_0/I_n *vs.* [Q] plots have been obtained.

$$I_0/I_n = A + B[Q] \quad (1)$$

In Fig. 1, the quenching equation was Eq. (2).

$$I_0/I_n = 0.998 + 2.24 \times 10^3\ [\textbf{PTZ-12}] \quad (r = 0.999) \quad (2)$$

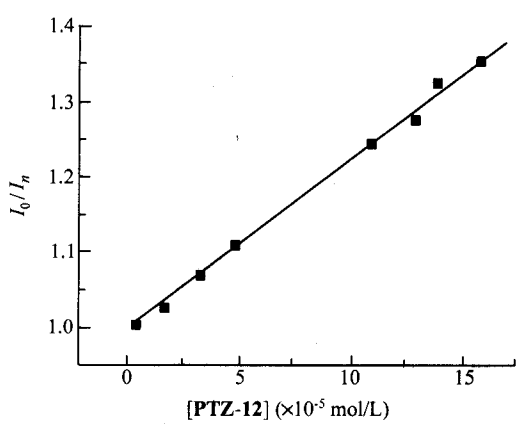

Fig. 1 I_0/I_n of **Pe-4*** (1×10^{-7} mol/L) *vs.* different [**PTZ-12**] $\times 10^{-5}$ mol/L plot at $\Phi = 0.36$ DX-H_2O at 35℃.

In Fig. 2, the quenching equation was Eq. (3) for **Fc-12-2**.

$$I_0/I_n = 0.9913 + 5.260 \times 10^4\ [\textbf{Fc-12-2}] \quad (r = 0.9996) \quad (3)$$

In Fig. 2, for **Fc-16-2** the quenching equation was Eq. (4).

$$I_0/I_n = 1.005 + 4.616 \times 10^4\ [\textbf{Fc-16-2}] \quad (r = 0.997) \quad (4)$$

Eq. (3) and Eq. (4) are very similar to Eq. (2). If we designate B as the slope of an I_0/I_n *vs.* [Q] plot, then an empirical B value can be evaluated by plotting I_0/I_n against the concentrations of the quencher [Q], for example in Fig. 2 $B = 5.26 \times 10^4$ mol^{-1}·L. Results of these B values measured at graded ϕ values in DX-H_2O systems are summarized in Table 1 to 5 for **Pe-n*** with different quenchers, *i.e.*, **PTZ-12** or **Fc-m** or **Fc-m-2**.

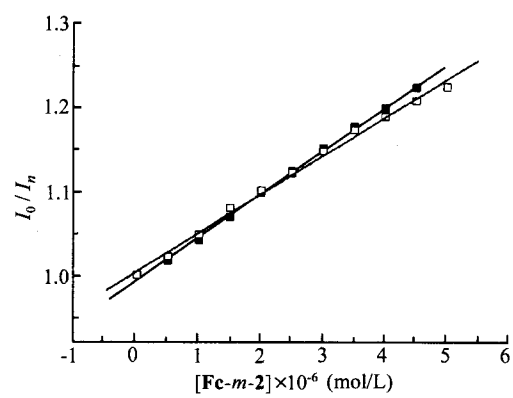

Fig. 2 I_0/I_n of **Pe-8*** (4×10^{-8} mol/L) *vs.* different [**Fc-12-2**] $\times 10^{-6}$ mol/L (or different [**Fc-16-2**] $\times 10^{-6}$ mol/L) plots in $\Phi = 0.36$ DX-H_2O at 35℃ ($m = 12$ (■) and $m = 16$ (□).

Table 1 B values (10^4 mol^{-1}·L) for the fluorescence quenching of **Pe-8*** at different fixed concentrations (mol/L) of **Pe-8** by **PTZ-12** as the quencher in 0.4 Φ DX-H_2O system at 35℃

[**Pe-8**]	1×10^{-7}	2×10^{-7}	3×10^{-7}	4×10^{-7}	5×10^{-7}
B	2.15	2.09	2.01	2.13	2.21

The uncertainty of B values is less than ± 10%.

Table 1 shows that at fixed concentrations of **Pe-8**

ranging from 1×10^{-7} mol/L to 5×10^{-7} mol/L, which is less than its CAgC value of 9.67×10^{-7} mol/L in 0.4 Φ DX-H_2O system,[14] the B values of the quenching process of **Pe**-8* by **PTZ-12** are constant when the experimental uncertainty is ± 10%. In other words, when [**Pe**-8] is smaller than its CAgC, B is a constant independent of [**Pe**-8].

Table 2 B values (10^4 mol^{-1}·L) for the fluorescence quenching of **Pe**-n* of different chain-length by **PTZ-12** as the quencher in DX-H_2O of different Φ values at 35℃

Pe-4	Φ	0.30	0.32	0.34	0.36	0.38	0.40
	B	0.816	0.475	0.359	0.224	0.161	0.106
Pe-8	Φ	0.34	0.36	0.38	0.40	0.42	0.44
	B	7.66	4.53	2.84	1.83	1.29	0.790
Pe-12	Φ	0.45	0.46	0.47	0.48	0.49	0.50
	B	6.36	4.79	3.93	2.58	1.93	1.35

The uncertainty of B values is less than ± 10%.

By comparing B values of **Pe**-4, **Pe**-8, and **Pe**-12 at the same or roughly the same Φ value, Table 2 shows that there is a chain-length effect of **Pe**-n on the B values of the quenching process by **PTZ-12** in coaggregates. The B value increases with the increase of the chain-length of the substituent group of **Pe**-n. In other words, the molecule with longer chain-length of the substituent group of **Pe**-n has a larger coaggregating tendency. Furthermore, log$B$ values of **Pe**-n* quenched by **PTZ-12** depend on the Φ values of DX-H_2O system and there was a linear relations between log$B$ and Φ.

It has been demonstrated quite a few times previously that there is a chain-foldability effect on aggregating tendency caused by HLI-driven self-folding of a longer chain.[17-19] This may lead to rather unexpected observations on chain-length effect, *e. g.*, a "double-chained" 16 carbon chain derivative might be found to have a smaller tendency toward aggregation than that of "double-chained" 8 carbon chain. This phenomenon has been sometimes rationalized by the concept of the chain-foldability effect of HLI. This is first exemplified in Table 3 by comparing B values at Φ = 0.20 for **Pe**-4*/**Fc**-12 and **Pe**-4*/**Fc**-16. More interestingly, there is a complete reversal of the chain-length effect when B values of **Pe**-4*/**Fc**-8-**2**, **Pe**-4*/**Fc**-12-**2** and **Pe**-4*/**Fc**-16-**2** at ϕ = 0.20 are compared. It indicated that the coaggregation tendency is **Fc**-8-**2** > **Fc**-12-**2** > **Fc**-16-**2** because larger B value signifies greater coaggregation tendency. It is interesting to note that the coaggregation tendency might be greatly affected by the chain-foldability of **Fc**-m-**2** driven by HLI. Data from Table 4 clearly showed that the aggregating tendencies or B values of the shorter "double-chained" 12-carbon derivative **Fc**-12-**2** at different Φ values ranging from 0.30 to 0.36 are always larger than those of the longer "double-chained" 16-carbon compound **Fc**-16-**2**. All these observations appear to be consequences of the chain-foldability effect.

In Table 4 and Table 5 show that the B values for **Pe**-8* or **Pe**-12* quenched by **Fc**-16 or **Fc**-12-**2**, or **Fc**-16-**2** depend on Φ values, *i. e.*, on the SAgP of the media. In a given aquiorgano system, the SAgP (an inherent solvent property) can be raised by decreasing the Φ values. It is expected that the lower the Φ value, the greater should be the B value of the fluorescence quenching of **Pe**-n* by the quencher. Therefore, B values for the ET fluorescence quenching process in coaggregates depend not only on the chain-length of the substituent group of **Pe**-n and the quencher but also on the SAgP of the media. Results of Table 4 shows that B values decrease linearly with increasing Φ according to Eq. (5) [for **Pe**-8*/**Fc**-16], (6) [for **Pe**-8*/**Fc**-12-**2**] and Eq. (7) [for **Pe**-8*/**Fc**-16-**2**] at Φ values ranging from 0.30 to 0.36.

$$\log B = -10.42\Phi + 8.23 \quad (r = 0.998) \quad (5)$$

$$\log B = -8.61\Phi + 7.82 \quad (r = 0.999) \quad (6)$$

$$\log B = -7.16\Phi + 7.26 \quad (r = 0.998) \quad (7)$$

Fig. 3 shows that there is a temperature effect on

the ET fluorescence quenching process brought about by the coaggregation for $\log B$, *i.e.*, $\log B$ values decrease linearly with increasing temperature according to the Eq. (8)

$$\log B = 5.59 - 0.0211T \quad (r = 0.997) \quad (8)$$

This is in accord with the established fact that aggregating tendencies of aggregators tend to decrease with increasing temperature.[20]

Table 3 B values (10^4 mol^{-1}·L) for the fluorescence quenching of **Pe-n*** of different chain-length by **Fc-m** or **Fc-m-2** as the quencher in DX-H_2O of different Φ values at 35℃

		Fc-4	Fc-8	Fc-12	Fc-16	Fc-4-2	Fc-8-2	Fc-12-2		Fc-16-2
Pe-4	Φ			0.20	0.20		0.20	0.20		0.20
	B	–	–	6.06	4.02	–	6.63	5.05		4.27
Pe-8	Φ		0.30	0.30	See		0.30	See		See
	B	–	0.628	2.52	Table 4	–	2.29	Table 4		Table 4
Pe-12	Φ				0.44			0.44	0.45	See
	B	–	–	–	1.17	–	–	3.61	1.70	Table 5

The uncertainty of B values is less than ± 10%.

Table 4 B values (10^4 mol^{-1}·L) for the fluorescence quenching of **Pe-8*** by **Fc-16** (or **Fc-12-2** or **Fc-16-2**) as the quencher in DX-H_2O of different Φ values at 35℃

	Φ	0.30	0.31	0.32	0.33	0.34	0.35	0.36
Fc-16	B	12.24	10.45	8.08	6.25	4.97	3.93	2.85
Fc-12-2	B	17.84	13.90	11.37	9.60	7.97	6.45	5.26
Fc-16-2	B	12.86	10.61	9.32	7.80	6.67	5.80	4.62

The uncertainty of B values is less than ± 10%.

Table 5 B values (10^4 mol^{-1}·L) for the fluorescence quenching of **Pe-12*** by **Fc-16-2** as the quencher in DX-H_2O of different Φ values at 35℃

Φ	0.44	0.45	0.46	0.47	0.48	0.49	0.50
B	8.33	6.21	4.89	3.77	2.99	2.30	1.75

The uncertainty of B values is less than ± 10%.

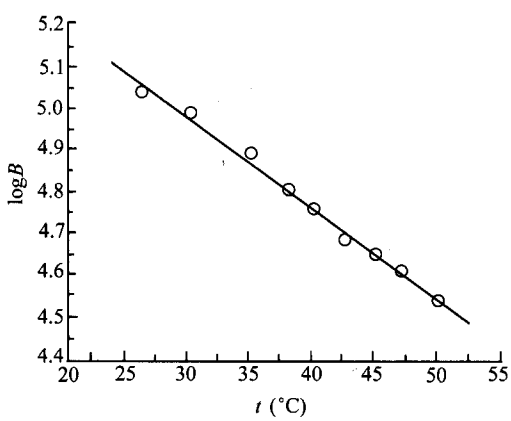

Fig. 3 $\log B$ *vs.* temperature plots for the fluorescence quenching of **Pe-8*** by **Fc-12-2** in $\Phi = 0.34$ DX-H_2O.

In conclusion, the acceleration of ET fluorescence quenching process between **Pe-n*** as the acceptor and **PTZ-12** (or **Fc-m**, or **Fc-m-2**) as the donor-quencher brought about by coaggregation under the influence of HLI has been demonstrated. Some novel results of the fluorescence quenching between **Pe-n*** and **Fc-m** or **Fc-m-2** in this case have been obtained. Organometallic compounds such as ferrocene derivatives are interesting compounds because of their ET properties. Experimental results show that the fluorescence quenching of **Pe-n*** by **Fc-m** is rather similar to that by *N*-alkylsubstituent phenothiazine.

Reference

1 Wasielewski, M. R. *Chem. Rev.* **1992**, *92*, 435.

2 Gust, D.; Moore, T. A.; Moore, A. L. *Acc. Chem. Res.* **1993**, *26*, 198.

3 Hagfeldt, A.; Gratzel, M. *Chem. Rev.* **1995**, *95*, 49.

4 Balzani, V. *Supramolecular Photochemistry*, Reidel, Dordrecht, Netherlands, **1987**.

5 Guldi, D. M.; Maggini, M.; Scorrano, G.; Press, M. *J. Am. Chem. Soc.* **1997**, *119*, 974.

6 Shi, J. L.; Chen, X.; Jiang, X. K. *J. Org. Chem.* **1996**, *61*, 4698.

7 Shi, J. L.; Qui, Z. H.; Jiang, X. K. *J. Phys. Org. Chem.* **1999**, *12*, 735.

8 Shi, J. L.; Yi, H. N.; Xu, J. Y.; Jiang, X. K. *Chin. J. Chem.* **2000**, *18*, 6.

9 Rosenblum, M. *Chemistry of the Iron Group Metallocenes*, John Wiley & Sons, Inc., **1965**.

10 Rochow, E. G.; Hurd, D. T.; Lewis, R. N. *The Chemistry of Organometallic Compounds*, John Wiley & Sons, Inc. **1957**, pp.244-249.

11 Riddik, J. A.; Bungeer, W. B.; Sakano, T. K., *Organic Solvents*, Vol. 2, 4th Ed; Techniques of Chemistry; Wiley-Interscience publication: New York, **1986**, 939.

12 Zeiger, H. E.; Rosenkranz, J. E. *J. Org. Chem.* **1964**, *29*, 2469.

13 Yi, H. N.; Shi, J. L.; Qiu, Z. H.; Xu, J. Y.; Jiang, X. K. *Chin. Chem. Lett.* **1999**, *10*, 839.

14 Shi, J. L.; Xu, J. Y.; Yi, H. N.; Jiang, X. K. *Chin. J. Chem.* **2000**, *18*, 617.

15 (a) Jiang, X. K. *Acc. Chem. Res.* **1988**, *21*, 362 and pertinent references cited therein.
(b) Jiang, X. K. *Pure Appl. Chem.* **1994**, *66*, 1621.

16 Lowry, T. H.; Richardson, K. S. *Mechanism and Theory in Organic Chemistry*, 3rd Ed; Harper & Row, New York **1987**, p. 232.

17 Jiang, X. K.; Hui, Y. Z.; Fan, W. Q. *J. Am. Chem. Soc.* **1984**, *106*, 3839.

18 Jiang, X. K.; Ji, G. Z.; Nie, J.; Zhang, J. T. *Chin. J. Chem.* **1991**, *9*, 559.

19 Jiang, X. K.; Zhang, J. T. *Aggregation and Self-Coiling of Organic Molecules*, Shanghai Science and Technique Press, Shanghai, **1996**, pp.118-124.

20 Zhang, J. T.; Jin, N.; Sun, S. X.; Ji, G. Z.; Jiang, X. K. *Chin. J. Chem.* **1994**, *12*, 179.

(E200009203 SONG, J.P.; LING, J.)